Transportation Research Part B 73 (2015) 13–33

Contents lists available at ScienceDirect

Transportation Research Part B

journal homepage: www.elsevier.com/locate/trb

GHG-emission models for assessing the eco-friendliness of road and rail freight transports

Thomas Kirschstein [a,*], Frank Meisel [b]

[a] School of Economics and Business, Martin-Luther-University, Gr. Steinstr. 73, 06108 Halle, Germany
[b] Faculty of Business, Economics and Social Sciences, Christian-Albrechts-University Kiel, Olshausenstr. 40, 24098 Kiel, Germany

ARTICLE INFO

Article history:
Received 26 June 2014
Received in revised form 9 October 2014
Accepted 8 December 2014

Keywords:
Emission model
Intermodal rail/road transportation
Greenhouse gases

ABSTRACT

Intermodal rail/road transportation is an instrument of green logistics, which may help reducing transport related greenhouse gas (GHG) emissions. In order to assess the environmental impact of road and rail transports, researchers have formulated very detailed microscopic models, which determine vehicle emissions precisely based on a vast number of parameters. They also developed macroscopic models, which estimate emissions more roughly from few parameters that are considered most influential. One of the goals of this paper is to develop mesoscopic models that combine the preciseness of micro-models while requiring only little more information than macro-models. We propose emission models designed for transport planning purposes which are simple to calibrate by transport managers. Despite their compactness, our models are able to reflect the influence of various traffic conditions on a transport's total emissions. Furthermore, contrasting most papers considering either the road or the rail mode, we provide models on a common basis for both modes of transportation. We validate our models using popular micro- and macroscopic models and we apply them to artificial and real world transport scenarios to identify under which circumstances intermodal transports actually effect lower emissions. We find that travel speed and country-specific energy emission factors influence the eco-friendliness of intermodal transports most severely. Hence, the particular route chosen for a transnational intermodal transport is an important but so far neglected option for eco-friendly transportation.

1. Introduction

Energy, in its various forms such as electricity and heat, is required for almost all social and economic activities in modern societies. A large part of the required energy is generated by combusting fossil fuels such as coal, natural gas or crude oil. Problematically, the combustion of fossil fuels also produces environmentally harmful emissions. These by-products can be categorized into greenhouse gases (e.g. carbon dioxide, methane, nitrogen dioxide) and air pollutants (e.g. nitrogen oxide, sulphur dioxide), see IPCC (2006). Greenhouse gases (GHGs) are considered responsible for the anthropogenic global warming whereas air pollutants are toxic and cause e.g. the acidification of soils and the eutrophication of waters. The transportation of freight and passengers is a major source of such emissions being responsible for about 14–22% of all GHG emissions (IPCC, 2014). The largest part of these emissions is caused by road transportation, which is why political efforts promote

* Corresponding author. Tel.: +49 (0) 345 5523 424; fax.: +49 (0) 345 5527 198.
E-mail addresses: thomas.kirschstein@wiwi.uni-halle.de (T. Kirschstein), meisel@bwl.uni-kiel.de (F. Meisel).

http://dx.doi.org/10.1016/j.trb.2014.12.004
0191-2615/

more eco-friendly transportation modes like rail or ship. However, using eco-friendly vehicles like trains or ships in the main haulage of a transport process usually calls for drayage transportation by truck, which often includes a detour compared with direct door-to-door shipping by road transportation. Therefore, intermodal transports are considered a key to eco-friendly transportation (Black et al., 2003), but it needs to be determined under which conditions they actually effect lower emissions than a unimodal road transport.

To account for the environmental effect of unimodal and intermodal transports, reliable models are needed for estimating the transport-related consumption of fuel or energy and for calculating the corresponding GHG emissions. Those emissions that directly result from the consumption of fuels within a transport are called tank-to-wheel (TTW) emissions (McKinnon and Piecyk, 2010). However, to achieve a fair comparison of fuel-driven and electric-driven vehicles, also the so-called well-to-tank (WTT) emissions caused by the production and distribution of a unit of fuel (respectively electricity) need to be taken into account. The sum of TTW and WTT yields the total well-to-wheel (WTW) emissions, which are a proper instrument for decision makers to compare the GHG emissions of different transport solutions. In order to determine the total emissions of a freight transport operation, the consumed amount of fuel respectively electricity needs to be known, which actually requires to estimate the physical energy that is required for the transport process.

In this paper, we provide emission models for rail and road transports based on an estimation of the energy demand of freight trains and trucks. In contrast to the already available models, our models are designed such that they include just those factors (speed, weight, traffic conditions, etc.) that influence the energy demand most. To model the effect of traffic conditions, a compact formulation for a vehicle's acceleration energy demand is introduced. The obtained advantage is that the models deliver more accurate estimates than established models. At the same time, both models are set up such that they can be parameterized easily by haulage managers. To reach this goal, we provide in Section 2 an overview on key concepts for measuring emissions of transport processes and we review the available literature on emission models for rail and road transports. Section 3 describes the developed emission models for trucks and freight trains. Section 4 validates the proposed emission models by comparing their results with existing emission models. In Section 5 our models are used for identifying those factors that influence the emissions of intermodal and unimodal transports most. In order to show additional degrees of freedom in planning urban unimodal and transnational intermodal transports, Section 6 provides two case studies. Section 7 concludes the paper.

2. Review of estimation models for transport-related GHG emissions

To assess the eco-friendliness of a transport operation, the amount and the composition of emitted GHGs have to be quantified. For making different types of GHGs comparable, a so-called CO_2 equivalence factor (CO_2e) is defined for each of them (IPCC, 2007). This factor expresses the global warming potential of one unit of a GHG compared with one unit of CO_2. E.g. Methane has a CO_2e-factor of 25, i.e. one ton of Methane has the same global warming effect as 25 tons of CO_2 (Edwards et al., 2014). Since combusting one liter of a fossil fuel effects particular amounts of certain types of GHGs, the amount of CO_2e per liter of a certain fuel type is fix. These so-called emission coefficients k are shown for diesel and fuel oil in Table 1. The table also shows the energy coefficient p, i.e. the amount of fuel that needs to be combusted for providing one kWh of energy to the transport process.

Given these emission coefficients and the total amount of fuel consumed by a vehicle (truck, plane, ship, or diesel locomotive) in a transport operation, the resulting total emissions are directly derived by multiplication. For vehicles with external energy supply, like electric cars or locomotives, the energy consumed within the transport process needs to be multiplied by a WTW emission coefficient that expresses the amount of GHG emitted for generating the consumed electricity. This coefficient varies from country to country as it depends on whether electricity is produced by nuclear power, coal power, wind power, etc. or a mixture thereof.

Calculating emissions from the amount of fuel or electricity consumed in a transport operation is referred to as the *consumption-based* emission calculation approach (Schmied and Knörr, 2013). This approach is suitable for transports that took place already. However, for the eco-oriented planning of future transports, GHG emissions have to be estimated based on specific data such as the vehicle to be used, the distance of the projected route, and the expected speed. For this purpose, numerous estimation models have been proposed in the literature but mostly for road transportation, see Demir et al. (2011, 2014). These models are categorized into *microscopic models* and *macroscopic models*. Microscopic models estimate fuel consumption and emissions very precisely. They use numerous vehicle-specific and trip-specific characteristics for a detailed simulation of the physics of the moving vehicle and the energy demand expected for a transport process. More specifically, the vehicle's speed during the trip (the so-called driving cycle) is analyzed to compute the driving resistances,

Table 1
Emission coefficients and energy coefficients (Schmied and Knörr, 2013)

	Emission coefficient k (kg CO_2e/l)		Energy coefficient p (l/kWh)	
	TTW	WTW	TTW	WTW
Diesel	2.49	3.15	0.1000	0.0811
Fuel oil	3.15	3.41	0.0889	0.0816

Table 2
Emission models proposed in the literature.

Microscopic models	Macroscopic models
Road	
CMEM (Scora and Barth, 2006)	EcoTransIT (Knörr et al., 2010)
PHEM (Hausberger et al., 2009; Rexeis et al., 2005)	HBEFA (Hausberger et al., 2009)
CPFCM (Rakha et al., 2011)	MEET (Hickman et al., 1999)
	COPERT (Kouridis et al., 2011)
Rail	
ARTEMIS (Lindgreen and Sorenson, 2005b)	EcoTransIT (Knörr et al., 2010)
	IFEU (Knörr et al., 2010)
	MEET (Jørgensen and Sorenson, 1997)

engine power output, and transmission losses at each point in time. If, however, the exact driving cycle is unknown, as is the case in a planning situation, an artificial driving cycle is assumed. Unfortunately, using artificial driving cycle data within a microscopic model actually reduces the informational value of the complex computations. In contrast, macroscopic models just roughly estimate emissions using a few parameters of a projected transport process, such as expected average speed and distance. Table 2 summarizes the most prominent models for road and rail vehicles in both categories. Selected models are described in more detail.

A prominent microscopic model for road transportation is the "Comprehensive Modal Emissions Model (CMEM)" of Scora and Barth (2006). The model is used in a simplified version in various pollution routing problems where vehicles are routed with the goal of minimum emissions, see e.g. Ramos et al. (2014), Franceschetti et al. (2013), and Bektaş and Laporte (2011). Since real driving cycle data is not available at the time of the transportation planning, the pollution routing problems feed the CMEM model with a trivial artificial driving cycle of constant speed $\bar{v}$. In other words, these routing models completely ignore any acceleration and deceleration processes. In the following this approach is called the simplified CMEM (sCMEM). These models then merely adjust the constant speed to improve the eco-friendliness of a route. For example, Franceschetti et al. (2013) approximate heavy traffic situations by assuming an average speed of 10 km/h which meets the specifications of stop&go situations on motorways quite well (Hausberger et al., 2009). However, in a stop&go situation low average speed results from a multitude of acceleration and deceleration processes (André, 2004), which effects much higher fuel consumption and emissions compared to moving traffic that flows at such a speed. This is because the energy that is spent for acceleration is lost each time that the vehicle comes to a stop (Hausberger et al., 2009). Therefore, such models need to be extended by a parameter that captures different traffic conditions (see also the conclusion in Bektaş and Laporte, 2011).

A microscopic model for trains is presented by Lindgreen and Sorenson (2005b). The model has been developed as part of the European ARTEMIS project (Boulter and McCrae, 2007). Similar to the road models, the train model is based on a calculation of physical driving resistances. This, however, is severely complicated by the length and the heterogeneous loading pattern of a train. For example, the number and type of railcars as well as the shape of their load are significant drivers of air resistance. In order to estimate emissions, the model does not describe the trip of a train by a continuous driving cycle (as in the road case) but by a discrete number of acceleration-speed combinations. By considering a set of realistic acceleration-speed combinations, a train trip is then characterized by a sequence of such combinations and the driving time spent on each of them. Like in the road case, this information is hardly available for a not yet performed trip, which makes it difficult to apply the model for planning future transport operations.

There also exist numerous macroscopic emission models. A prominent example is the EcoTransIT framework (Knörr et al., 2010; Schmied and Knörr, 2013), which has been proposed for road and rail transports in Europe. The road model relies on the "Handbook of Emission Factors for Road Transport" (HBEFA) (Hausberger et al., 2009), which in turn is based on the microscopic PHEM model. It considers the truck type, the load weight, the road profile (flat, hilly, mountainous) and the road type (motorway, urban road etc.) as parameters. A web-application EcoTransIT (2014) has been set up for applying the model easily to European transport routes, which, however, restricts the road type to motorways and the road profile to a specific value for each country (e.g., Germany is considered hilly, Switzerland is mountainous, etc.). The model roughly estimates the expected fuel consumption rate f_j (in l/km) of a truck of type j depending on the payload quantity m^{load} (in t), the fuel consumption rate r_j^{base} of the empty truck, the additional fuel consumption r_j^{add} of the fully loaded truck, and the payload capacity m_j^{cap} as

$$f_j(m^{\text{load}}) = r_j^{\text{base}} + r_j^{\text{add}} \cdot \frac{m^{\text{load}}}{m_j^{\text{cap}}}. \tag{1}$$

For calculating the energy consumption of a freight train, EcoTransIT takes into account the type of traction, the payload and the rail track profile. For example, the energy consumption rate e (in Wh/km) of an electric train of total weight m (in t) on a hilly track is estimated based on empirical data by

$$e(m) = 1200 \cdot m^{0.38}. \tag{2}$$

This function is intended for trains with a total weight in the range $[600, 2200]$. For larger trains, a constant value $e = 22$ kWh/km is assumed. For flat and mountainous tracks, a 10% reduction or surcharge is used. For diesel trains, (2) is simply divided by an efficiency value of 0.37.

More detailed macroscopic models for road and rail are provided by the MEET project (Hickman et al., 1999; Jørgensen and Sorenson, 1997). Here, the emissions of a road vehicle are expressed as a function of average speed for various vehicle types, which is then further corrected concerning varying payloads and also road gradients, see Demir et al. (2014) for further details. A freight train's energy consumption is estimated by (3) which also considers the train's average speed $\bar{v}$, its maximum speed $v^{\max}$ (both in m/s), the trip length d (in km), the number of accelerations to maximum speed n^{acc}, and the difference in altitude over the trip h (in m) by

$$e(m, \bar{v}, v^{\max}, d, n^{\text{acc}}, h) = \frac{m}{3.6} \cdot \left(\frac{n^{\text{acc}}}{2 \cdot d} \cdot v^{\max} + 24.7 + 0.845 \cdot \bar{v}^2 + 9.81 \cdot \frac{h}{d} \right). \tag{3}$$

Regarding the usefulness of available emission models for transportation planning, the brief literature review on existing emission models results in two fundamental conclusions:

(a) Microscopic emission models require too detailed information about the trip that is yet to be planned. For example, a trip's speed curve is unknown ex ante. If these models are used for transportation planning, simplifications are necessary such as assuming a constant speed and neglecting acceleration processes. Therefore, no reliable estimation of emissions can be expected from such models.
(b) Macroscopic emission models derive from empirical data bases functions for estimating average emission rates. These approaches capture some of the relevant planning parameters (e.g. payload and, sometimes, speed) but neglect others (such as traffic conditions). Furthermore, the underlying data base must be kept up to date to reflect technological development and the models are not adjustable for individual variations of technological parameters.

Hence, to properly judge on the emissions of alternative transport options, transportation managers require mesoscopic emission models that capture the most relevant planning parameters using only little information on the alternative transport opportunities while being sufficiently detailed for an easy adoption to technological variations.

3. Mesoscopic emission models

3.1. Base model

In order to develop our mesoscopic models, we start from a very fundamental consumption based approach. Let f be the amount of fossil fuel consumed by a vehicle within a transport process. The associated emissions GHG are calculated by multiplying f with the corresponding WTW emission coefficient k that expresses the amount of CO_2e emitted from burning one unit of fuel (see Table 1). For liquid fuels whose consumption f is measured in liter, emissions GHG are then computed by

$$\overset{[\text{gGHG}]}{\text{GHG}} = \overset{[\text{l}]}{f} \cdot \overset{\left[\frac{\text{gCO}_2\text{e}}{\text{l}}\right]}{k}. \tag{4}$$

Eq. (4) is the basis of the consumption-based emission estimation approach described in Section 2. If, however, the considered transport operation is just about to be planned, the amount of fuel f is yet unknown to the planner. It can then be estimated by

$$\overset{[\text{l}]}{f} = \overset{[\text{kWh}]}{W} \cdot \overset{\left[\frac{\text{l}}{\text{kWh}}\right]}{p} \cdot \overset{[-]}{\frac{1}{\epsilon}}. \tag{5}$$

Here, W is the expected total energy required for moving the vehicle along its route, p is the quantity of fuel that provides one kWh, and coefficient $\epsilon = \epsilon^e \cdot \epsilon^t$ reflects the efficiency of the combustion engine (ϵ^e) and the powertrain (ϵ^t) in terms of the fraction of the fuel's chemical energy that is actually transformed into kinetic energy of the vehicle. Exemplary values of p are shown in Table 1. As will be shown later in this section, W can be estimated from physical properties of the vehicle, the characteristics of the route, the expected driving speed, and the expected traffic conditions. From (4) and (5), emissions GHG can be computed by

$$\overset{[\text{gCO}_2\text{e}]}{\text{GHG}} = \overset{[\text{kWh}]}{W} \cdot \frac{1}{\epsilon} \cdot \overset{\left[\frac{\text{l}}{\text{kWh}}\right]}{p} \cdot \overset{\left[\frac{\text{gCO}_2\text{e}}{\text{l}}\right]}{k}. \tag{6}$$

Eq. (6) can also be applied to electric vehicles, such as electric locomotives. For this purpose, we simply drop p and we redefine k (now measured in $\frac{[\text{gCO}_2\text{e}]}{[\text{kWh}]}$) as the WTW emission rate of the electric power that drives the vehicle.

Since p, k, and ϵ are merely parameters (physical or provided by the vehicle manufacturers), the only challenge of applying (6) lies in determining W. This energy can be calculated by physical rules of a thermodynamical system which transforms the chemical energy of the fuel into kinetic energy of the vehicle. More precisely, W is calculated by determining the power

that is needed to overcome the four main forces, namely (i) rolling resistance, (ii) air drag, (iii) grade, and (iv) inertia, that occur during a movement. For calculating these energy requirements, we primarily follow the notion of Ross (1997) and Scora and Barth (2006). The power P^{roll} that is required to overcome rolling resistance is calculated by

$$P^{\text{roll}}(m, v) \approx c^{\text{roll}} \cdot \overset{\left[\frac{\text{m}}{\text{s}^2}\right]}{g} \cdot \overset{[\text{t}]}{m} \cdot \overset{\left[\frac{\text{m}}{\text{s}}\right]}{v} \tag{7}$$

where c^{roll} denotes the rolling resistance coefficient, g is the gravitational acceleration (i.e. $g = 9.81\ \frac{\text{m}}{\text{s}^2}$), m is the vehicle's total weight, and v is the speed. To overcome air resistance, the required power P^{air} is calculated by

$$P^{\text{air}}(v) = \frac{1}{2000} \cdot c^{\text{air}} \cdot \overset{\left[\frac{\text{kg}}{\text{m}^3}\right]}{\rho} \cdot \overset{[\text{m}^2]}{A} \cdot \overset{\left[\frac{\text{m}^3}{\text{s}^3}\right]}{v^3} \tag{8}$$

where c^{air} is the drag coefficient, ρ is the air density (i.e. $\rho = 1.2\ \frac{\text{kg}}{\text{m}^3}$) and A is the area of the vehicle's front surface. To overcome the grade, power P^{grade} is computed by

$$P^{\text{grade}}(m, v, i) \approx \overset{[\text{t}]}{m} \cdot \overset{\left[\frac{\text{m}}{\text{s}^2}\right]}{g} \cdot \overset{\left[\frac{\text{m}}{\text{s}}\right]}{v} \cdot i \tag{9}$$

where i is the track's grade in percent. Inertia is overcome by power P^{inert} as

$$P^{\text{inert}}(m, v) = \frac{1}{2} \cdot \overset{[\text{t}]}{m^{\text{inert}}} \cdot \overset{\left[\frac{\text{m}}{\text{s}^2}\right]}{a} \cdot \overset{\left[\frac{\text{m}}{\text{s}}\right]}{v} \tag{10}$$

where a denotes the acceleration and m^{inert} is the inertial mass. Ross (1997) assumes $m^{\text{inert}} = 1.03$ m. To calculate a trip's total energy consumption, the total power level needs to be integrated over the trip's duration

$$\overset{[\text{kWh}]}{W} = \int_{t=t_1}^{t_2} P(v(t), a(t), i(t), m)dt \tag{11}$$

where $P(v(t), a(t), i(t), m) = P^{\text{roll}}(\cdot) + P^{\text{air}}(\cdot) + P^{\text{grade}}(\cdot) + P^{\text{inert}}(\cdot)$. The time indices t_1 and t_2 indicate the begin and the end of the vehicle movement. Please note that the power functions in (7)–(11) only consider mass m, speed v, and grade i as input variables, whereas also physical and technical parameters like c^{roll} and A could be considered as arguments. Anyhow, we take the perspective of a transport manager who is in charge of determining a route for a given type of vehicle. Hence, m, v and i can be influenced whereas c^{roll}, A, etc. are fixed parameters.

Problematically, solving (11) ex ante is difficult because the variation of speed and the accelerations during a trip depend on many aspects such as traffic conditions and driving characteristics. Clearly, these factors are stochastic processes which realize just during the trip. Nevertheless, expectations about the traffic conditions on a particular route are often known, for example in terms of historical or even up-to-date traffic information. An emission model should be capable of including such information to obtain reliable results. Further parameters such as average speed and vehicle load depend on the decisions of the transport manager. Hence, a useful emission model should be able to account for both, the emission-relevant exogenous traffic conditions (represented in terms of the expected number of accelerations per driven kilometer) and the manager's decisions regarding vehicle speed and load.

Among all influencing factors, acceleration requires most energy, in particular in heavy traffic. Unfortunately, it is also very difficult to assess this type of energy. Therefore, in the following subsections, we spend effort on developing a common framework for approximating the acceleration energy required by trucks and trains within a transport process.

3.2. Truck emissions model

For long-haul truck transports on free highways, acceleration phases are comparatively rare. Hence, most emission models (such as sCMEM and EcoTransIT) discard the effect of accelerations on emissions. In urban traffic and in heavy traffic situations, however, acceleration occurs very frequently. Next to the number of acceleration processes, also the speed variation within each of these accelerations determines the total energy demand. Therefore, an acceleration function needs to be known for calculating the energy demand. Nie and Li (2013) present a compact formulation for acceleration energy demand assuming a constant acceleration a. However, as a vehicle's acceleration depends on power supply and power demand, we follow Rakha and Lucic (2002) and treat acceleration as a variable. It can be expressed as the difference of the vehicle's effective tractive force F and the driving resistance $P^{\text{drive}} = P^{\text{air}} + P^{\text{roll}} + P^{\text{grade}}$ by

$$a(v) = \frac{F(v)}{m \cdot 1,000} - \frac{P^{\text{drive}}(v)}{m \cdot v}. \tag{12}$$

According to Rakha and Lucic (2002), the tractive force F can be computed by

$$\overset{[\mathrm{N}]}{F}(v) = \min\left(1000 \cdot \epsilon^t(v) \cdot \frac{P^{\text{vehicle}}}{v}\,;\, g \cdot m^{\text{trac}} \cdot \mu\right). \tag{13}$$

The first expression in the min(·) function computes the tractive force depending on the power of the vehicle's engine P^{vehicle} (in kW) and on the vehicle's power transmission efficiency $\epsilon^t(v)$ depending on v. The second expression is an upper bound, which avoids that $F \to \infty$ in case that $v \to 0$. This value depends on the load m^{trac} of the tractive axle(s) and the friction coefficient μ. Following Rakha and Lucic (2002), we approximate the tractive axle's load by $m^{\text{trac}} = m \cdot 0.35$. For $\epsilon^t(v)$, we suggest the following continuous approximation of the non-continuous functions proposed in Rakha and Lucic (2002) and Rexeis et al. (2005)

$$\epsilon^t(v) = 0.88 - 0.72 \cdot e^{-0.077 \cdot v^{1.41}} \tag{14}$$

where v is the vehicle speed in km/h. Fig. 1 depicts the functions provided by Rakha and Lucic (2002) (with $v_0 = 20$ and $\epsilon^t_0 = 0.88$) and Rexeis et al. (2005) as well as our approximation for $v \in [0, 25]$. Fig. 1 implies that (14) captures the shape of the efficiency function of Rexeis et al. (2005) quite well but avoids the discontinuity at $v \sim 20$ km/h such that (14) yields a smooth transmission efficiency function. Such a smooth transmission efficiency function yields a smoother function of acceleration energy consumption which eases approximation of the latter.

With these definitions, the acceleration function depends on the vehicle's speed, the mass and other coefficients. As the acceleration (12) is the derivative of speed w.r.t. time and speed is the derivative of the distance traveled w.r.t. time, a second-order ordinary differential equation (ODE) is constituted by

$$a(v) = y'' = \frac{F(y')}{m \cdot 1000} - \frac{P^{drive}(y')}{m \cdot y'} \tag{15}$$

where y is the distance traveled. Since $F(v)$ is non-continuous, a straight-forward analytic solution is not possible. Therefore, numerical solution methods have to be applied. To calculate the distance function as well as its first and second derivative (i.e. $a(\cdot)$ and $v(\cdot)$), the ODE is solved with the parameters shown in Table 3.

The acceleration work is then computed by

$$W^{\text{inert}}(v, m) = \frac{1}{2 \cdot 3600} \cdot m^{\text{inert}} \int_{v_t^{-1}(v_1)}^{v_t^{-1}(v_2)} (a(\tau, m) \cdot v(\tau, m))\, d\tau \tag{16}$$

based on the ODE solutions. To approximate (16), ODEs are solved for $m = \{14, 20, 26, 32, 38, 40\}$ tons. A good fit to the ODE solutions results from the following function:

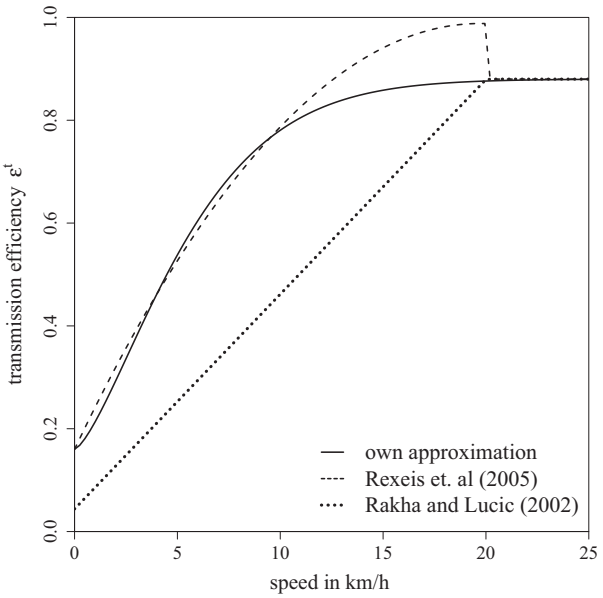

Fig. 1. Approximation of transmission efficiency for trucks.

Table 3
Parameters for trucks (Rakha and Lucic, 2002; Rexeis et al., 2005).

Parameter	c^{air}	c^{roll}	ϵ_0^t	A	P^{vehicle}	μ
Value	0.6	0.006	0.88	9 m^2	300 kW	0.6

$$\widehat{W}^{\text{inert}}_{\text{truck}}(v,m) = \frac{0.504}{2\cdot 3600}\cdot m\cdot v^2 \tag{17}$$

which estimates the energy needed for a single acceleration process from 0 to speed v. Fig. 2 shows the fitted function and the ODE results for a truck of $m = 30$ tons. It can be taken from this figure that the approximation (17) of truck acceleration energy delivers a convincing fit.

The actual number of acceleration processes faced within a trip depends on the traffic conditions. We denote by n^{acc} the average number of acceleration processes per kilometer driven by the vehicle. Typical values for n^{acc} are 1–4 for urban trips and 0.1–0.2 for highway trips, see De Haan and Keller (2004) and André (2004). Then, the total energy necessary to move the truck over a distance d is approximated based on (11) as

$$\begin{aligned}\overline{W}^{[\text{kWh}]}_{\text{truck}}(d,m,\bar{v},\bar{i}) &= \frac{d}{\bar{v}}\cdot\left(P^{\text{roll}}(\bar{v},m)+P^{\text{air}}(\bar{v})+P^{\text{grade}}(\bar{v},\bar{i},m)\right)+n^{\text{acc}}\cdot d\cdot\widehat{W}^{\text{inert}}_{\text{truck}}(\bar{v},m)\\ &= \frac{d}{\bar{v}}^{[\text{h}]}\cdot P^{\text{drive}}(\bar{v},m,\bar{i})^{[\text{kW}]}+n^{\text{acc}}\cdot d\cdot\widehat{W}^{\text{inert}}_{\text{truck}}(\bar{v},m)^{[\text{kWh}]}.\end{aligned} \tag{18}$$

The energy estimated by (18) for moving the vehicle is then used in (6) together with the efficiency ϵ to estimate the CO_2e emissions of a trip.

As shown above, a vehicle's transmission efficiency declines for low speeds. Similarly, engine efficiency ϵ^e declines for low power outputs due to imperfect combustion and friction. ϵ^e is typically expressed as the specific fuel consumption rate (in g/kWh). The fuel consumption rates of a vehicle are summarized in (non-linear) fuel consumption- or efficiency-maps which quantify the relation between engine speed (measured in rpm) and power demand on the fuel consumption rate (whereby the engine speed is affected by the gear chosen). Standardized fuel consumption maps based on various truck types are provided by Rexeis et al. (2005). These maps indicate that the following linear relation between an engine's fuel consumption rate and the engine's power demand is a reasonable simplification

$$\frac{1}{\epsilon^e} = \left(\frac{r^{\text{idle}}}{P^{\text{dem}}}+\frac{r^{\text{full}}-r^{\text{idle}}}{P^{\text{vehicle}}}\right)\cdot\frac{1}{p} = \left(r^{\text{idle}}\cdot\left(\frac{1}{P^{\text{dem}}}-\frac{1}{P^{\text{vehicle}}}\right)+\frac{r^{\text{full}}}{P^{\text{vehicle}}}\right)\cdot\frac{1}{p} \tag{19}$$

where P^{vehicle} is the engine's (maximal) power, r^{idle} is the truck's fuel consumption rate (in l/h) if idle, and r^{full} at full power. P^{dem} is the average (instantaneous) power demand during the trip calculated as

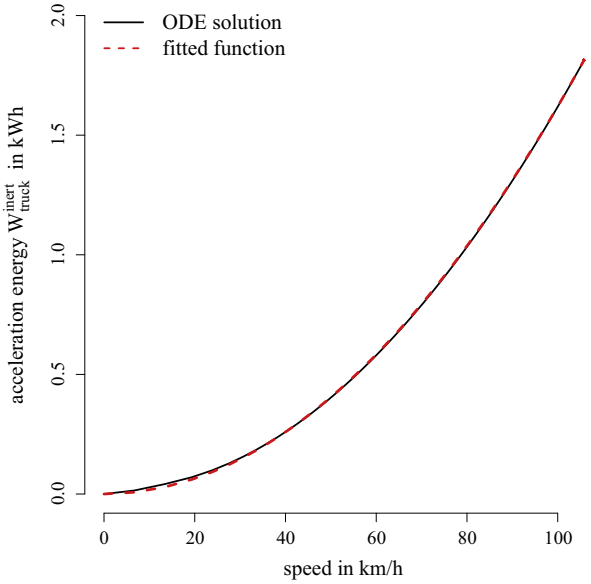

Fig. 2. Acceleration energy required by a truck ($m = 30$ t) for reaching speed v.

$$P^{\text{dem}}(d,m,\bar{v},\bar{i}) = \frac{1}{\epsilon^t(v)} \cdot \left(P^{\text{drive}}(m,\bar{v},\bar{i}) + n^{\text{acc}} \cdot d \cdot \widehat{W}^{\text{inert}}_{\text{truck}}(\bar{v},m) \cdot \frac{\bar{v}}{d} \right). \tag{20}$$

Note that the ratio $\frac{r^{\text{full}}}{P^{\text{vehicle}}}$ typically corresponds to the engine's point of optimal fuel efficiency. Considering a recent truck with $P^{\text{vehicle}} = 300$ kW engine, an optimal fuel consumption rate of $\frac{r^{\text{full}}}{P^{\text{vehicle}}} = 0.229$ l/kWh and an idle consumption rate of $r^{idle} = 3$ l/h can be assumed. These values are used in the following calculations.

In combination, the CO_2e emissions of a road transport can be calculated using (6) by plugging in the corresponding values of the necessary work (based on (18)) and the average efficiency (as the product of (19) and (14)). After some algebra, it holds

$$\text{GHG}_{\text{truck}} = k \cdot \left(\frac{d}{\bar{v}} \cdot r^{\text{idle}} + \frac{(r^{\text{full}} - r^{\text{idle}})}{\epsilon^t(\bar{v}) \cdot P^{\text{vehicle}}} \cdot \overline{W}_{truck}(d,m,\bar{v},\bar{i}) \right). \tag{21}$$

3.3. Freight train emissions model

The driving resistances of freight trains are determined by other factors than those being relevant for trucks. For example, the rolling resistance of trains is expected to be quite low because both, wheels and tracks, are made of steel. However, the resistance increases with the number of wheels of a train such that it is actually dependent on the number of railcars attached to the train. This needs to be reflected by the rolling coefficient c^{roll}, which is part of (7). Lindgreen and Sorenson (2005a) provides the following formula to calculate such a coefficient for a freight train

$$c^{\text{roll}}_{\text{train}} = c^{\text{roll}}_{\text{loc}} \cdot \frac{m_{\text{loc}}}{m} + c^{\text{roll}}_{\text{car}} \cdot \frac{m_{car}}{m} + \frac{n_{\text{axles}}}{10 \cdot m \cdot g} + c^{\text{roll}}_{\text{aux1}} \cdot \frac{v}{100} + c^{\text{roll}}_{\text{aux2}} \cdot \left(\frac{v}{100}\right)^2 \tag{22}$$

where m_{loc} is the locomotive's deadweight, m_{load} is the total weight of railcars (including payload), and n_{axles} is the total number of axles of the train. All other coefficients are constants for particular types of locomotives and railcars, see the exemplary values in Table 4.

The air resistance of trains depends not only on the front surface of the locomotive but also on the number and the surface of the attached railcars. In general, air resistance increases with increasing train length. Following Lindgreen and Sorenson (2005a) the air resistance coefficient c^{air} for a (homogeneously loaded) train is

$$c^{\text{air}}_{\text{train}} = c^{\text{air}}_{\text{loc}} + n_{\text{cars}} \cdot c^{\text{air}}_{\text{car}} \tag{23}$$

where n_{cars} is the number of railcars attached to the train. Furthermore, the loading pattern of a train and, thus, the turbulences due to gaps between railcars, also increase air resistance. However, we neglect this effect here for reasons of simplicity.

To estimate the acceleration energy for a freight train, we apply the same basic approach as for the truck model of Section 3.2. Here, we solve ODEs for trains with payloads $m_{\text{load}} = \{200, 300, \ldots, 1200\}$ tons. The train's total weight is calculated by assuming a payload capacity of 60 t per railcar, a tare weight of 20 t per railcar and a locomotive weight of 83 t. Hence, the trains' total weights are $m = \{363, 483, \ldots, 1683\}$. The approximation of a train's acceleration energy results in function (24). The function fits again excellently to the ODE solution as is shown in Fig. 3.

$$\widehat{W}^{\text{inert}}_{\text{train}}(v,m) = \frac{0.52}{2 \cdot 3600} \cdot m \cdot v^2. \tag{24}$$

To compute a train's total energy demand, we replace in (18) $\widehat{W}^{\text{inert}}_{\text{truck}}$ by $\widehat{W}^{\text{inert}}_{\text{train}}$ and obtain

$$\overline{W}^{[\text{kWh}]}_{\text{train}}(d,m,\bar{v},\bar{i}) = \frac{d}{\bar{v}}^{[\text{h}]} \cdot \left(P^{\text{roll}}(\bar{v},m) + P^{\text{air}}(\bar{v})^{[\text{kW}]} + P^{\text{grade}}(\bar{v},\bar{i},m) \right) + n^{\text{acc}} \cdot d \cdot \widehat{W}^{\text{inert}}_{\text{train}}(\bar{v},m)^{[\text{kWh}]}. \tag{25}$$

To compute a train trip's total emissions, also the type of traction and the efficiency of the energy supply system matter. Both aspects are captured in (6) by parameters ϵ, p, and k. For diesel traction, the parameters p and k are basically the same as for truck transports. However, no studies on the efficiency of diesel locomotives in situations with low energy demand are available. Instead, Lindgreen and Sorenson (2005b) report total efficiency levels for diesel locomotives of about $\epsilon = 38\%$. I.e. for diesel trains, the total emissions are computed as

$$\text{GHG}^{\text{diesel}}_{\text{train}} = \frac{\overline{W}_{\text{train}}(d,m,\bar{v},\bar{i})}{\epsilon} \cdot p \cdot k. \tag{26}$$

Table 4
Parameters for a train with a 4-axle locomotive carrying fully loaded container railcars (Lindgreen and Sorenson, 2005a).

Parameter	$c^{\text{air}}_{\text{loc}}$	$c^{\text{air}}_{\text{car}}$	$c^{\text{roll}}_{\text{loc}}$	$c^{\text{roll}}_{\text{car}}$	$c^{\text{roll}}_{\text{aux1}}$	$c^{\text{roll}}_{\text{aux2}}$
Value	0.8	0.218	0.003	0.0006	0.0005	0.0006

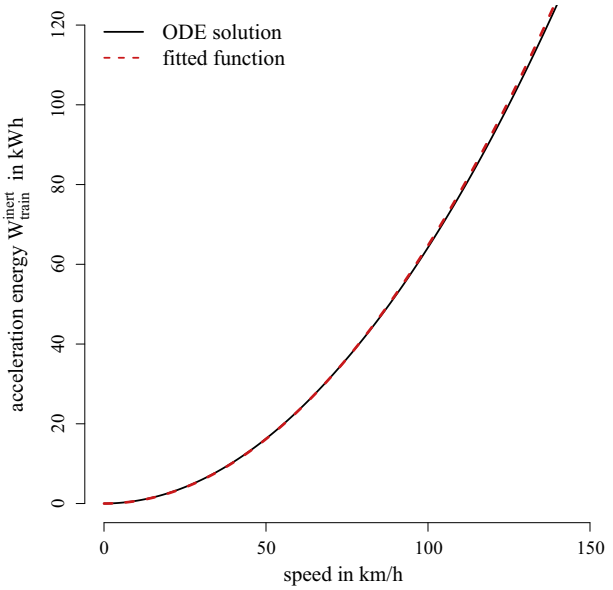

Fig. 3. Acceleration energy required by a train ($m = 1163$ t) for reaching speed v.

Electric locomotives have a higher total efficiency of about $\epsilon = 65\%$ (Lindgreen and Sorenson, 2005b). The WTW emission coefficient k for such trains varies from country to country, depending on the efficiency of the energy supply system and the country's energy mix. For example, Schmied and Knörr (2013) report a WTW emission coefficient of $k = 0.574\ \frac{kgCO_2e}{kWh}$ for Germany. In general, we then calculate an electric train's emissions by

$$GHG^{elec}_{train} = \frac{\overline{W}_{train}(d, m, \bar{v}, \bar{i})}{\epsilon} \cdot k. \tag{27}$$

4. Validation of the models

4.1. Truck

We validate the model proposed in Section 3.2 by comparing its emission rates with reference values used in practice. As a reference, we use the macroscopic model codified in the European norm EN 16258, see Schmied and Knörr (2013). As test setting, we consider a fully loaded truck (payload = 26 t, total weight $m = 40$ t) which conducts a loaded travel of 100 km in combination with a drayage of 60 km traveling empty. The macroscopic model estimates a WTW emission rate of 63 gCO_2e/tkm for this transport operation, see Schmied and Knörr (2013).

In order to apply our model, we use the truck parameters provided in Table 3. For the empty trip of the truck, we take the rolling resistance coefficient of $c^{roll} = 0.0076$ reported in Rexeis et al. (2005). We assume an average speed of 83 km/h, which is the average highway speed used to calculate emission factors in HBEFA. As further input, the number of accelerations n^{acc} is set to 0.12 per km, which approximates different traffic conditions on an average highway trip. Using these values and the diesel figures of Table 1, our model (21) estimates an emission rate of 61 gCO_2e/tkm. This value is just slightly below the emission rate reported by Schmied and Knörr (2013). The deviation is explained by the fuel consumption of about 0.37 l/km assumed in Schmied and Knörr (2013), which is comparatively high as this value also includes stop&go and urban traffic conditions. In contrast, Rexeis et al. (2005) report fuel consumptions of 0.25–0.28 l/km for pure highway trips.

The norm EN 16258 is also implemented within the online-tool EcoTransIT (2014) where it is combined with geographical information to compute emission rates for real-world transport relations. We test a transport scenario where a fully loaded truck with $m = 40$ tons travels within Germany from the city of Halle to the city of Leipzig. This corresponds to a road travel distance of $d = 37$ km, for which EcoTransIT (2014) reports a total WTW energy consumption of 178 kWh. Since the cities' altitudes are 87 m and 110 m we apply $i = 0.062\%$ within our model. In EcoTransIT (2014) highway conditions are assumed for all trips, which corresponds to average speeds of $\bar{v} = 83$ km/h for trucks in Germany. Since the considered trip also contains a substantial share of urban roads, we set $n^{acc} = 0.2$ for our model. With these inputs and the further parameters of Tables 1 and 3, we compute a total WTW energy of 181 kWh, which is also very close to EcoTransIT (2014). If, however, the assumed speed is considered too high for this trip, one may also consider a more reasonable speed like $\bar{v} = 40$ km/h. Here, our model estimates an energy consumption of 133 kWh. Obviously, the speed and traffic conditions heavily influence the total emissions. Therefore, an emission model like ours, which accounts for both these effects, is expected to deliver more reliable emission values that offer better transport planning capabilities.

We further validate our model by comparing its results under varied speed (for a truck of constant total weight $m = 40$ t) and varied truck load (for fixed speed $v = 50$ km/h) to the results of the macroscopic model of the norm EN 16258 (Schmied and Knörr, 2013; EcoTransIT, 2014) and the sCMEM, i.e. the simplified microscopic model of Scora and Barth (2006) as it is used e.g. by Bektaş and Laporte (2011). Fig. 4a shows the total CO_2e emissions of the truck if traveling over a distance of $d = 100$ km at various speeds. Fig. 4b shows the emissions if the truck travels at constant speed $v = 50$ km/h whereas the payload takes different values. All other parameters are set as before. The two figures reveal that speed and payload influence the total CO_2e emissions differently. CO_2e emissions depend non-linearly on speed. The optimal speed with minimal emissions is about 40 km/h. Below this speed, the engine operates inefficiently. Above this speed, the air drag effects a quadratic increase of emissions. Though (8) suggests a cubic effect of speed on emissions the effect reduces to quadratic order due to the multiplication of the average energy level with the expected travel time $\frac{d}{v}$, see Eq. (18). In contrast, emissions grow linearly if the payload increases (Fig. 4b). Corresponding emissions per tkm are shown in Fig. 4c/d. Note that the emissions per tkm decrease in Fig. 4d because of the increasing payload. From the four plots in Fig. 4 it can be seen that the compared models capture the effect of truck weight precisely. However, the impact of speed is not captured in Schmied and Knörr (2013)

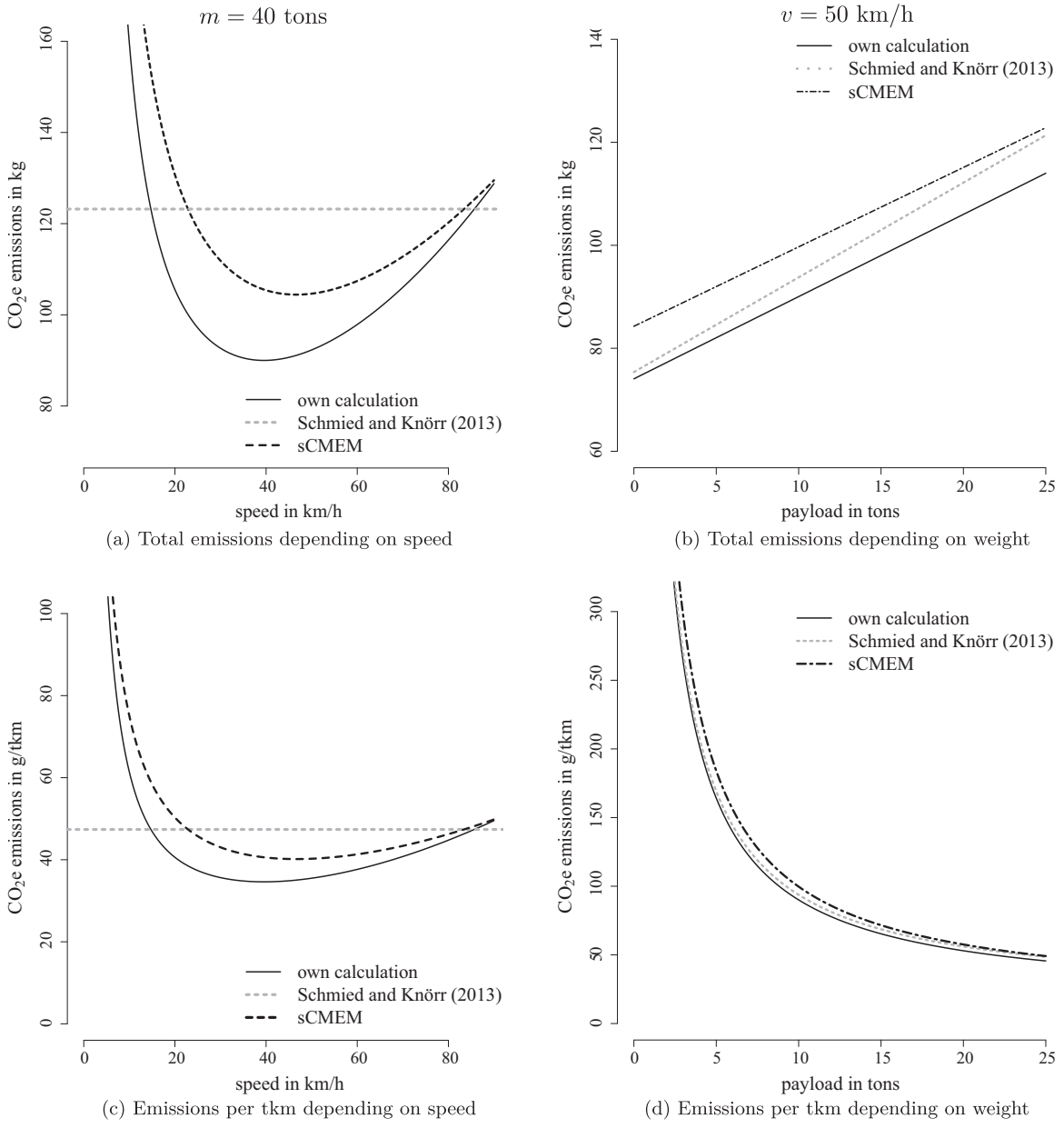

(a) Total emissions depending on speed

(b) Total emissions depending on weight

(c) Emissions per tkm depending on speed

(d) Emissions per tkm depending on weight

Fig. 4. Emissions of a truck depending on speed and payload.

and EcoTransIT (2014), because these approaches rely on a preset default speed. Since the parameter has a significant impact on the emissions, it is questionable whether these approaches are useful for planning transport operations with regard to GHG emissions. The effect of speed on emissions is captured in the sCMEM and in the model presented here. This shows that our model achieves the goal of precisely estimating emissions at a reasonable computational effort, similar to sCMEM but much simpler than CMEM.

Together, the combined non-linear interrelation of a truck's load and its speed w.r.t. total CO_2e emissions is shown in Fig. 5. It becomes obvious that the interplay of payload and speed determines the total CO_2e emissions. Hence, both parameters can be used for influencing the CO_2e emissions of a transport process in a desired way. The modeling approach described in this paper allows the proper quantification of this trade-off for a specific planning situation.

4.2. Train

To validate the train model, we consider a freight train with 20 railcars carrying 3 TEUs each. The train's total load is 1200 tons and the train's total weight is approximately 1833 tons. The average speed is assumed to be $v = 73$ km/h (Lindgreen and Sorenson, 2005b) and 4 stops are planned on a trip with 100 km length (i.e. $n^{acc} = 0.04$). With the parameters of Tables 1 and 4 and the emission rates for the German electricity supply system, we obtain from (25) an energy consumption of 0.019 kWh/tkm for an electric train and a diesel consumption of 0.005 l/tkm for a conventional train. Schmied and Knörr (2013) report for a heavy train corresponding values of 0.018 kWh/tkm and 0.005 l/tkm which supports the results of our model.

Lindgreen and Sorenson (2005b) report an empirical energy consumption for a freight train moving over a distance of 52.5 km between the Danish cities Kopenhagen and Køge. The train had a payload of 1368 tons and a total gross weight of 2146 tons. The authors report an energy consumption that corresponds to 0.048 kWh/tkm. They also present the microscopic ARTEMIS model for a precise estimation of freight train emissions. With an average speed of 73 km/h for freight trains in Denmark, the authors report an energy consumption of 0.073 kWh/tkm, which is far higher than the empirical observation. EcoTransIT (2014) computes for this trip an energy consumption of 0.034 kWh/tkm, which is far below the reported value. This result might by due to the geographical information system included in EcoTransIT, which estimates a travel distance of merely 48 km for the considered transport relation. In order to apply our model and without further information, we assume 4 stops on the trip (i.e. $n^{acc} = 0.076$). We compute an energy consumption of 0.046 kWh/tkm, which fits much better to the empirical values than the results of Lindgreen and Sorenson (2005b) and EcoTransIT (2014).

To illustrate the effect of payload and speed on energy consumption, Fig. 6 presents emission rates for a freight train with the above mentioned specifications over a trip of 100 km. For the settings with varied speed, we assume a constant payload of 900 t (about 15 fully loaded container railcars) and a total train weight of $m = 1283$ t. For the settings with varied weight, we assume a constant speed of 70 km/h. Figs. 6a and 6c show a quadratic relation between speed and emissions, similar to the truck results in Fig. 4a/c for speeds larger than 40 km/h. The macroscopic model of Schmied and Knörr (2013) provides emission rates only for a few selected payload classes. As shown in Fig. 6a/c these values are close to our model only if a (high) average speed is achieved within a transport process. Otherwise, the macroscopic model fails again as it does not

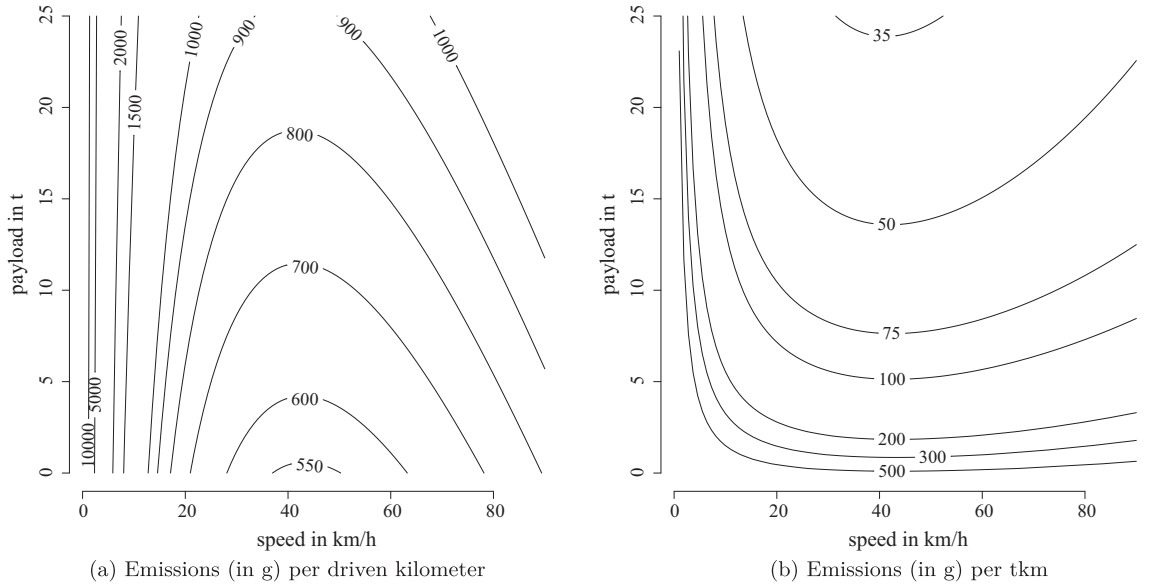

(a) Emissions (in g) per driven kilometer (b) Emissions (in g) per tkm

Fig. 5. CO_2e emissions of a truck depending on speed and payload.

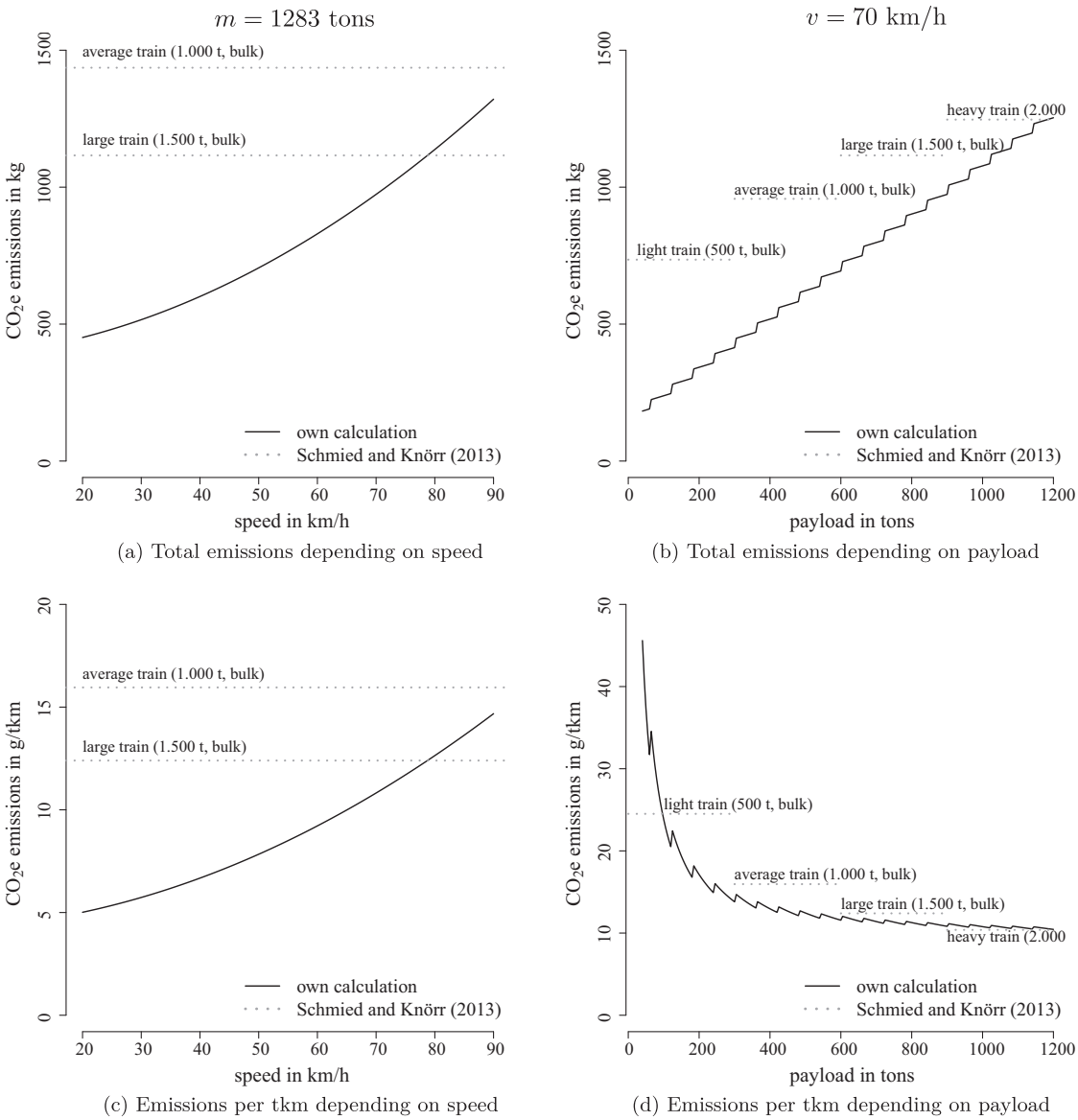

(a) Total emissions depending on speed

(b) Total emissions depending on payload

(c) Emissions per tkm depending on speed

(d) Emissions per tkm depending on payload

Fig. 6. Emissions of an electric train depending on speed and payload.

capture the effect of speed on emissions. Furthermore, according to Fig. 6b/d, the effect of payload is also captured only roughly by Schmied and Knörr (2013), because of the few train types considered in their model. Here, our model offers the advantage of capturing arbitrary payload values which is particularly relevant for light freight trains where emissions react drastically to the payload, see Fig. 6d. Note that the sawtooth patterns in Figs. 6b and 6d result from the successive attachment of new railcars for increasing payload, where each new railcar increases the number of axles and the train's tare weight. This effects a stepwise linear relation between payload and total CO_2e emissions, see Fig. 6. In contrast, the emission rates per tkm show a non-monotonously decreasing pattern, because adding a new railcar for a marginal amount of payload increases the average emissions per unit of payload, see Fig. 6d.

The interplay between payload and speed is depicted in Fig. 7. Again, the sawtooth pattern is striking, which illustrates the effect of attaching further railcars. The general relation between speed and payload to the emission rates is similar to the truck case. However, the contour lines in Fig. 7b show a steeper pattern which indicates that the emission rates per tkm for a train is influenced to a lower extent by the payload. In general, the emission rates per tkm are clearly lower for freight trains than for trucks. For highly utilized trains, only a forth of the truck emission rate is observed. Note that this factor relies on the characteristics of the German energy supply system. Countries with an energy mix that is more (less) eco-friendly achieve even better (worse) emission rates for trains.

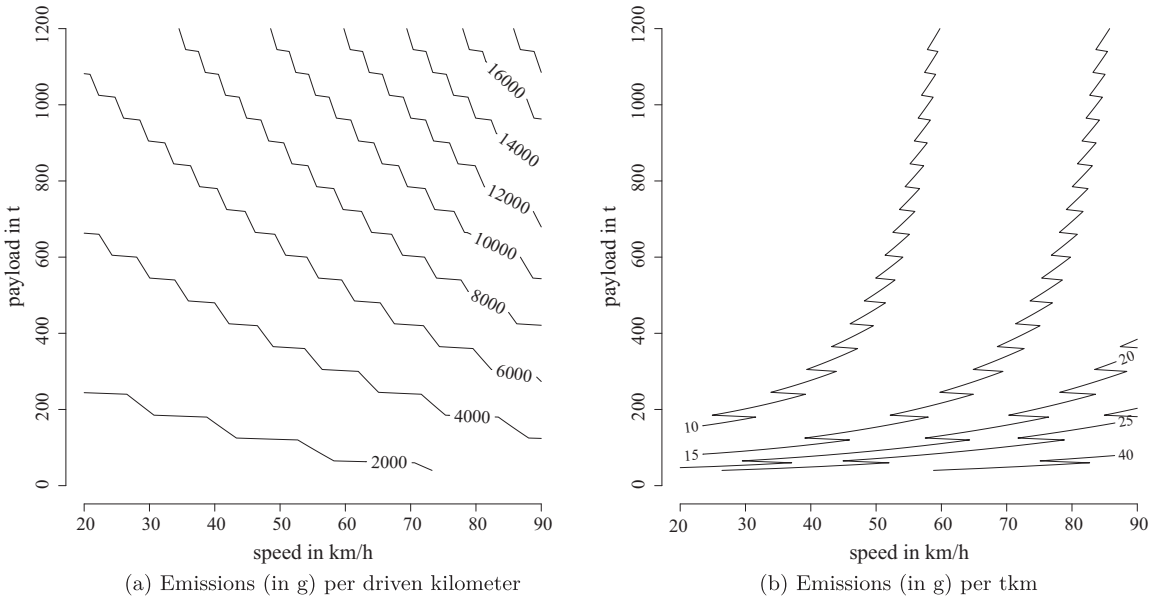

(a) Emissions (in g) per driven kilometer (b) Emissions (in g) per tkm

Fig. 7. CO_2e emissions of a train depending on speed and payload.

5. Assessing GHG emission drivers

5.1. Experimental design

In this section, we assess the competitiveness of intermodal rail/road transportation versus unimodal road transportation concerning GHG emissions in various transport settings. The goal is to identify the fundamental factors that determine whether or not an intermodal transport produces less emissions than a unimodal transport. For this purpose, we apply our emission models to one of the well known test instances of Solomon (1987), which were originally proposed for the capacitated vehicle routing problem with time windows (CVRPTW). We use here the test instance C1 which consists of a central depot and 100 customer locations that are grouped in clusters of 10 customers each. This data set provides us with customer locations, demand rates, and distances that serve all together as a basic transport scenario for which we determine unimodal and intermodal transport solutions under various settings. On the one hand, the used test instance is artificial which requires some systematic modifications to fit the demand rates and further parameters to a realistic transport setting. On the other hand, the artificial instance allows varying relevant parameters like distances and speed to identify the most relevant drivers of the CO_2e emissions in uni- and intermodal transportation. The following modifications are performed to adapt the test data to our needs:

1. The Euclidean distances derived from the original instance are interpreted as kilometers. Furthermore, the customer area is scaled up by multiplying the coordinates with 10 such that the distances represent long-distance transport relations as is an economic prerequisite for intermodal transportation.
2. The original demand values are divided by 10 and interpreted as tons. Hence, each cluster of customers demands a total of about 20 tons of freight which is roughly one truck load. Time windows and processing times are ignored.
3. A local depot is located at the center of each cluster. The depots serve as intermodal terminals for mapping rail/road transports onto this problem.

For the experiment, we distinguish four basic transport settings:

1. All customers are served by the central depot using trucks. Each cluster is served by one truck. The routing of the trucks minimizes the CO_2e emissions.
2. All customers are served by the central depot using trucks. Each cluster is served by one truck. The routing of the trucks minimizes the travel distance.
3. A train serves the local depots in a round-trip, whereas the local distribution within each cluster is performed by trucks at minimum CO_2e emissions.
4. A train serves the local depots in a round-trip, whereas the local distribution within each cluster is performed by trucks at minimum total travel distance.

In order to determine the truck routes for these solutions, classic traveling salesman problems (TSP) and emission-minimizing travel salesman problems (TSP^{emis}) are modeled in Appendix A and solved using the standard solver CPLEX 12.6 (IBM, 2014). The obtained solutions are illustrated in Fig. 8. The results are analysed subsequently.

5.2. Unimodal transports

We start by analyzing the unimodal road transport solutions with lowest total emission and lowest total distance, see Fig. 8a and c, respectively. Concerning the structure of these solutions, we observe that the truck routes are identical for almost all clusters (except for clusters I, III and VI), no matter whether travel distance or CO_2e emissions are minimized. The explanation is that any deviation from the distance-optimal route (for early visiting high demand customers and, thus, quickly reducing payload and CO_2e emissions) causes a detour that consumes additional fuel mostly countervailing the

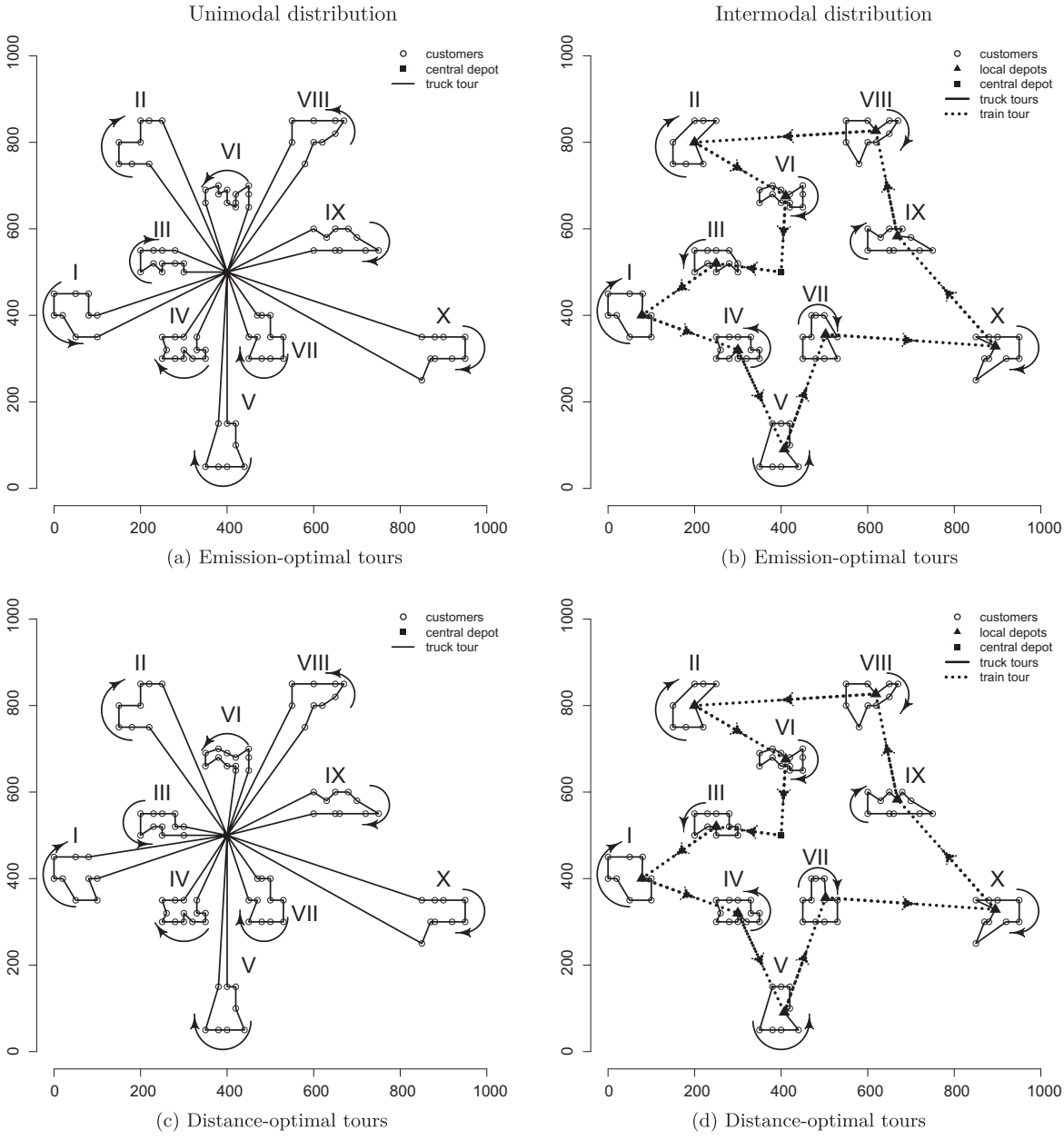

Fig. 8. Distance- and emission-optimal tours for uni- and intermodal distribution.

Table 5
CO_2e emissions and total travel distances for unimodal scenarios.

Avg. speed $\bar{v}$ (km/h)	CO_2e emission in kg		Total travel distance in km	
	Dist.-opt.	Emiss.-opt.	Dist.-opt.	Emiss.-opt.
40	5346	5341	8289	8305
50	5484	5478	8289	8298
60	5878	5871	8289	8298
70	6469	6461	8289	8295
80	7228	7220	8289	8295
90	8141	8132	8289	8295

intended reduction of CO_2e emissions. The overall difference in total travel distance and total emissions is less than 1% for the two solutions. This finding is in line with earlier studies (e.g., Kopfer et al., 2014).

The presented transport solutions have been derived assuming an average truck speed of $\bar{v} = 40$ km/h. The corresponding exact CO_2e emissions and travel distances of the distance- and the emission-optimal solution are provided in Table 5. The table also shows these measures for various higher speeds. As expected, CO_2e emissions strongly increase with increasing speed, whereas the distances are (almost) unaffected by the chosen speed. In any case, we observe that the speed of a vehicle does not affect the routing, no matter whether the goal is to minimize distance or emissions.

A further issue is the orientation of a route (indicated by arcs in Fig. 8). Since the distances are symmetric in this test setting, the travel distance is not affected by whether a truck processes the customers of a cluster clockwise or counterclockwise. However, the emissions can differ as the orientation of the route determines how the payload changes in the course of the service process, which has also been observed in Suzuki (2011). Therefore, in Fig. 8, the routes are orientated such that they effect least emissions. Now, if a planner would not care for this effect and select the opposite orientation for each of these routes, we observe a 3% increase of the total CO_2e emissions for the considered solutions.

Eventually, a planner might consider switching from conventional diesel to alternative fuels like biodiesel in order to reduce CO_2e emissions. The corresponding reduction potential is quite large, because conventional diesel causes 3.24 kg CO_2e WTW-emissions per liter whereas pure biodiesel emits only 1.92 kg CO_2e per liter (EcoTransIT, 2014). However, the reduction potential is limited as blended fuels with a large share of biodiesel (or even pure biodiesel) increase fuel consumption. Since such fuels are further suspected to boost engine corrosion, they have not been established in practice so far.

To summarize, this experiment confirms the strong dependency of emissions on the chosen speed and the orientation of a route. These appear as the most critical decisions regarding eco-friendliness in this case study. In contrast, the routing and, thus, the traveled distances remain unaffected by the chosen speed and the pursued objective.

5.3. Intermodal transports

In the intermodal setting, customers of a cluster are served from the local depot via truck. The local depots are supplied by an electric train that starts and ends its route at the central depot. Fig. 8b,d show the corresponding transport solutions with lowest emissions and lowest travel distance. We again observe identical routings except for the local distribution of clusters III and IV. The total travel distance in both solutions is about 6600 km where rail traffic accounts for about 3000 km. Therefore, we concentrate in the following on analyzing the CO_2e emissions of the two solutions. We assess the impact of the train's travel speed, the WTW emission coefficient of the electricity consumed, the total payload of the train, and the orientation of the route. We consider two speed values $\bar{v} = 50$ km/h and $\bar{v} = 70$ km/h. The WTW emission coefficients depend on the (mix of) energy sources used for producing electricity for the transport sector. We consider here emission coefficients of 0.574 kg/kWh, 0.077 kg/kWh, and 1.085 kg/kWh, which respectively correspond to the energy supply networks of Germany (DE), France (FR), and Poland (PL), see Schmied and Knörr (2013). For the payload, two scenarios are distinguished. In the "empty train" scenario the train's load consists only of the customer demand. As the total customer demand is merely 200 tons, the train's capacity utilization is quite low even at the beginning of the tour. This leads to comparatively high emissions per tkm because of the large dead weight of the locomotive. In contrast, in the "full train" scenario, we assume that the train carries not just the customer demand but also further cargo. We assume here an initial payload of 980 tons, which is about the average payload of freight trains in Germany, see Jørgensen and Sorenson (1997).

Table 6 reports the CO_2e emissions for the distance- and emission-optimal solutions of the introduced scenarios. As in the unimodal setting, the difference in total emissions between distance-optimal and emission-optimal transport solutions is negligibly small. The influence of average speed, however, is more remarkable. An increase in speed from 50 to 70 km/h increases the total emissions by about 20–30%. The most striking effect on the total emissions, however, results from the energy source of electricity in the specific countries. In France, CO_2e emissions are lowest for all settings due to a large share of nuclear power. In contrast, intermodal transports in Poland never emit less emissions compared to the unimodal transport even if the train is fully loaded. For Germany, an intermodal transport is eco-friendlier than a unimodal transport if the train is highly utilized. Note that in the intermodal scenarios, a basic value of emissions is caused by the truck's drayage tours in the clusters (independent of the country). This accounts for about 2000–2500 tons CO_2e for $\bar{v} = 50$ and $\bar{v} = 70$, respectively.

Table 6
Country-specific emissions (in kg) for intermodal transport scenarios.

	$\bar{v} = 50$ km/h		$\bar{v} = 70$ km/h	
	Dist.-opt.	Emiss.-opt.	Dist.-opt.	Emiss.-opt.
DE				
Full train	4417	4410	5558	5549
Empty train	7143	7136	9213	9204
FR				
Full train	2643	2636	3166	3157
Empty train	3009	3002	3656	3647
PL				
Full train	6240	6233	8018	8009
Empty train	11,393	11,386	14,927	14,919
Unimodal (see Table 5)	5484	5478	6469	6461

For all countries, the proportionate emissions of carrying the load of 200 t within a fully loaded train are about 57% lower than in the "empty train" setting. Furthermore, if the planner does not care about the orientation of the truck and train routes, the CO_2e emissions may increase by up to 6%.

To summarize this experiment, the most relevant factor in intermodal transportation is the country-specific energy emission coefficient which can differ by a factor of 10 or more even within a small geographical area like central Europe. Therefore, transport managers in charge of planning transnational transports are strongly advised to consider country-specific characteristics and to assess alternative routes if available. A further crucial factor is the load of a train which yields a strong motivation for consolidating large amounts of freight that utilize a train completely. The chosen speed has the lowest impact on the CO_2e emissions but, nevertheless, still accounts for up to 16% of the emissions. Altogether, the parameters of an intermodal transport solution have a much stronger impact on the CO_2e emissions compared with the unimodal transport.

6. Two case studies on the eco-friendliness in transportation planning for urban and international transport relations

6.1. Urban transport relation

In this section, we study the effect of different route choices in a city logistics setting. We compare a route that uses solely urban roads with a route that uses city highways for a delivery within a megacity. As a case study, we take the city of Berlin which has a dense network of urban roads and city highways. A truck has to carry two TEU with a total weight of 12.5 tons each from a freight rail yard in south-east Berlin to Tegel airport. The truck either takes the urban route via the city center or the highway route. Both routes are shown in Fig. 9.

The urban route traverses the city center at a total distance of 22.5 km. The highway route circles around the city center with a total travel distance of 29 km, composed of 26 km traveled on highways and 3 km traveled on urban roads. For urban

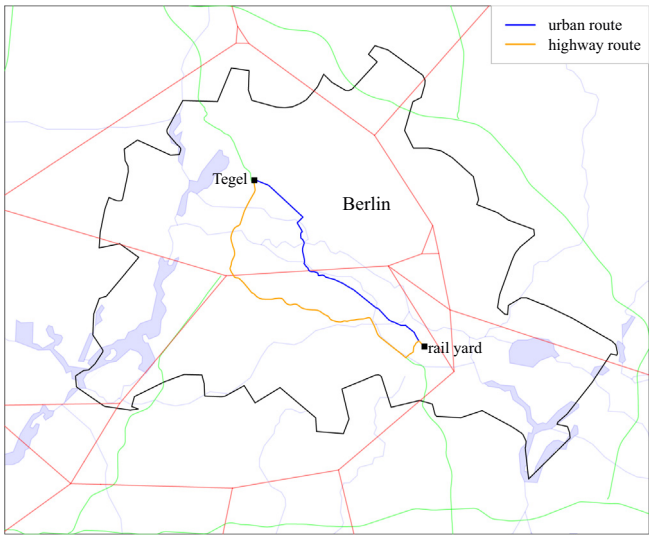

Fig. 9. Considered transport options between Tegel airport and the rail yard.

Table 7
Performance of two transport options between Tegel airport and the rail yard.

	CO_2e emissions (in kg)			Total distance (in km)
	Our model	sCMEM	EcoTransIT	
Urban route	43.6	**30.5**	**34.1**	22.5
Highway route	**40.1**	41.6	42.4	29.0

Emission-minimal transport option is set in bold for each model.

Table 8
Eco-performance of two route options for varied n^{acc}_{urban} ($n^{acc}_{highway} = 0.12$ is held constant).

n^{acc}_{urban}	Urban route		Highway route	
	CO_2e (in kg)	Share of acc. energy (%)	CO_2e (in kg)	Share of acc. energy (%)
0.12	25.8	3.5	37.7	8.7
1.0	32.4	23.2	38.6	10.7
1.5	36.1	31.2	39.1	11.6
2.0	39.9	37.7	39.6	12.2
2.5	43.6	43.0	40.1	12.8
3.0	47.4	47.5	40.6	13.3
3.5	51.2	51.4	41.1	13.7
4.0	54.9	54.7	41.6	14.0
4.5	58.7	57.6	42.1	14.3
5.0	62.4	60.2	42.6	14.6

roads, an average speed of $v_{urban} = 40$ km/h is assumed whereas for highways an average speed of $v_{highway} = 70$ km/h is assumed. Note that the urban route is the shorter one whereas the highway route is faster. We assume an acceleration frequency of $n^{acc}_{urban} = 2.5$ per km for urban roads, which is a moderate value for city trips, see De Haan and Keller (2004) or André (2004). For highways, we assume an acceleration frequency of $n^{acc}_{highway} = 0.12$ per km as was used before. Table 7 shows the emissions estimated for both routes with our model, the sCMEM model, and EcoTransIT (2014). For the calculations with EcoTransIT (2014), we assume a truck utilization of 100% and an empty trip factor of 0%. All further parameters are set as before. The results of Table 7 show that all models calculate similar emissions of about 41 kg for the highway route. However, for the urban route, sCMEM and EcoTransIT (2014) report much lower emissions of 30.5 kg and 34.1 kg, respectively. The reduction corresponds to the smaller travel distance of the urban route, where sCMEM additionally takes into account the lower travel speed whereas EcoTransIT (2014) assumes a constant speed. In contrast, our model reports higher emission rates which is because it considers the effect of traffic conditions (in terms of the higher number of acceleration processes) on the urban roads. This means that our model identifies the highway route as the preferable choice for minimizing emissions.

To further quantify the relevance of acceleration processes for a trip's emissions, Table 8 shows the total CO_2e emissions and the share of acceleration energy for varied values n^{acc}_{urban} of accelerations on the urban road segments of the two routes. It can be seen that a large number of accelerations (e.g. in an urban traffic jam) can easily cause more than 50% of total emissions. In the other extreme, under flowing highway traffic, still about 9% of total energy consumption accounts for acceleration. Hence, ignoring acceleration severely biases the estimation of emissions in any traffic situation. In this experiment, for any value $n^{acc}_{urban} \geqslant 2$, the highway route is to be preferred over the urban route w.r.t. the CO_2e emissions.

6.2. European transport relation

We investigate here the case of a European transport relation in order to estimate the role of country-specific energy emission coefficients for a real-world scenario. The transport involves carrying 20 TEU á 12.5 tons from the port of Hamburg to Bratislava, capital of Slovakia (SK). Three transport options are considered:

- road transport: 10 trucks each carrying 2 TEU directly from Hamburg to Bratislava.
- rail route #1: 1 electric train carries all TEU on a rail route via Czech Republic.
- rail route #2: 1 electric train carries all TEU on a rail route via Austria.

For the road transport, we consider a route of 983 km which is the shortest in the European highway network. We assume an average travel speed of 83 km/h, which corresponds to a net transport duration of about 12 h. For the rail transports, the first routing represents the shortest possible route (942 km) within the European rail network. This route goes via Prague where large parts of the trip take place in the Czech Republic (CZ). The second rail route (1079 km) goes from Hamburg

Table 9
Data of the considered routings.

	DE	CZ	AT	SK	Total
Distances (km)					
Road transport	545	378	–	60	983
Rail route #1:	495	383	–	64	942
Rail route #2:	775	–	282	22	1079
Emission coefficient k [kgCO_2e/kWh]	0.574	0.661	0.119	0.199	–

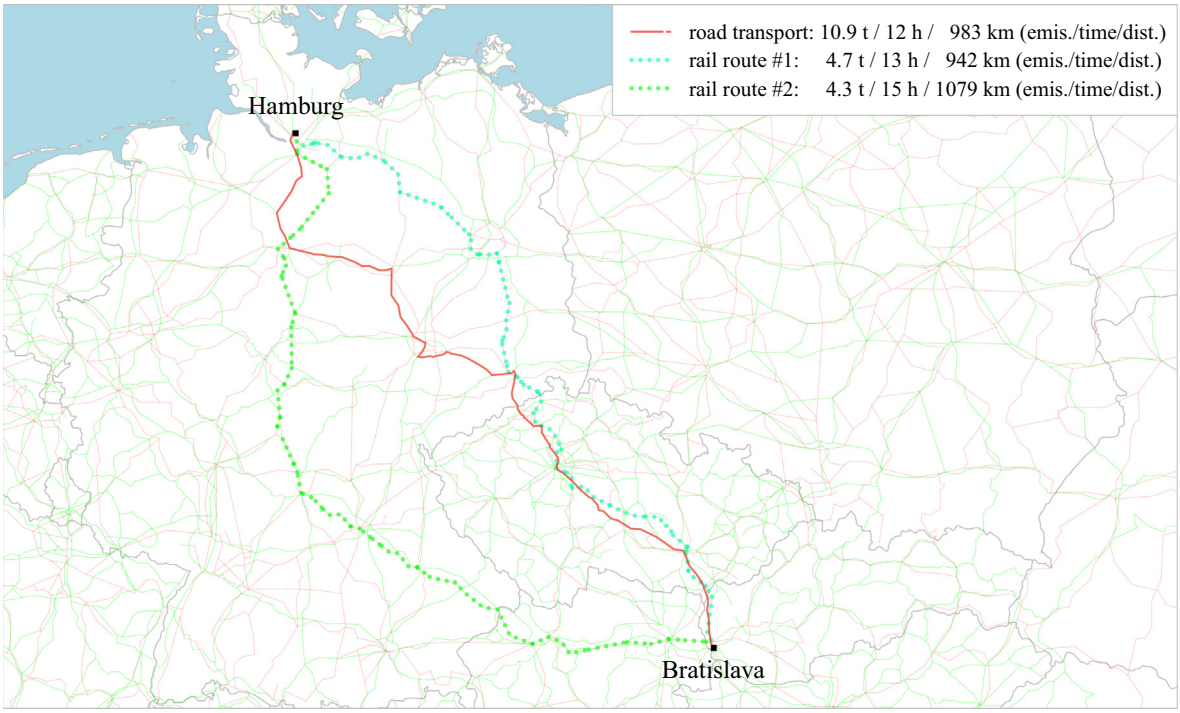

Fig. 10. Considered transport options between Hamburg and Bratislava.

to Bratislava via Passau and Vienna in Austria (AT). Table 9 summarizes the distances of the considered routes and the WTW emission coefficients for electricity in the involved countries. The latter are taken from Schmied and Knörr (2013).

Fig. 10 illustrates all three routes together with the expected travel time, the total distance, and the CO_2e emissions estimated by our models. Table 10 summarizes these performance measures as computed by our models and by EcoTransIT (2014). For the latter, we set an empty trip factor of 0%, a 100% capacity utilization for the trucks, and a total train weight of 448 t, which appropriately reflect the characteristics of the described transport scenarios.

The results presented in Table 10 and Fig. 10 show that both models deliver comparable results. Slight deviations in the computed emissions are explained by the fact that the geographical information system of EcoTransIT (2014) seems to choose slightly different routes as is revealed by the deviations in the total distances. Anyhow, both approaches identify rail route #2 as the best transport option concerning total CO_2e emissions. Both rail transport options emit only half of the emissions of the road transport despite the fact that a comparatively short train is used for which the dead weight is relatively

Table 10
Performance of three transport options for the relation Hamburg–Bratislava.

	CO_2e emissions (in t)		Total distance (in km)		Travel time (in h)	
	Our model	EcoTransIT	Our model	EcoTransIT	Our model	EcoTransIT
Road transport	10.9	10.0	983	930	12	11
Rail route #1	4.7	5.3	942	1007	13	14
Rail route #2	4.3	4.6	1079	1212	15	17

high. Among the two rail transport options, the eco-friendly route #2 is actually about 15% longer than route #1. Nevertheless, the additional emissions caused by the detour of route #2 are overcompensated by the reduction of emissions due to the comparatively favorable energy mix in Germany and Austria compared with the Czech Republic, see coefficients in Table 9. This case study shows clearly that the country-specific energy mix has to be taken into account when striving for eco-friendly transportation planning in an international environment. The models developed in this paper can be used for determining the environmental impact of alternative transport options as has been illustrated here for a real word example.

7. Conclusions

This paper proposes mesoscopic emission models for estimating the CO_2e emissions of road and rail transportation. The models account for relevant parameters such as travel speed, payload, and traffic conditions. They are more detailed than macroscopic emission models (which discard relevant parameters) and less complex than microscopic emission models (which require excessive input data). The models are validated by comparing them to various microscopic and macroscopic emission models as well as to empirical data. The results show that the CO_2e emissions are accurately estimated. For example, the proposed truck emission model achieves results similar to the microscopic CMEM model of Scora and Barth (2006), but it requires no calibration regarding engine friction. Furthermore, our model captures the impact of acceleration processes on the emissions without requiring trip-specific speed curves as an input. With this parameter, the model also captures the effect of different traffic conditions, which is important to differentiate e.g. highway trips from trips within an urban environment.

The scope of the developed models makes them a suitable tool for logistics managers who look for a compromise between preciseness and computational effort. The models can support transportation planning decisions, particularly the choice of eco-friendly means of transport, routes, and speeds. Tests with artificial transport scenarios show that speed and country-specific energy emission coefficients strongly affect the eco-friendliness of intermodal transports and, thus, the competitiveness of intermodal transportation against unimodal transportation. This finding is supported by a real world case study that compares different routing alternatives for a freight transport in Europe. Another case study on urban transportation confirms the impact that traffic conditions have on GHG emissions. Together, the experiments show that these features of our models can help to largely reduce the CO_2e emissions of short haul and (international) long haul transports in uni- and intermodal transportation.

Appendix A. TSP formulations

[If desired, the appendix can be transfered to an electronic appendix.]

We provide models for the classical distance-minimizing traveling salesman problem (TSP) and for an emission-minimizing traveling salesman problem (TSP^{emis}) using the notation shown in Table 11. The TSP model is based on Sherali and Driscoll (2002).

$$[\text{TSP}] \qquad \min \rightarrow \sum_{(i,j)\in\mathcal{E}} d_{ij}\cdot x_{ij} \tag{28}$$

$$\sum_{j\in\mathcal{V}} x_{ij} = 1 \qquad \forall i\in\mathcal{V},\quad i\neq j \tag{29}$$

$$\sum_{i\in\mathcal{V}} x_{ij} = 1 \qquad \forall j\in\mathcal{V},\quad j\neq i \tag{30}$$

$$\sum_{j\in\mathcal{C},j\neq i} y_{ij} + (n-1)\cdot x_{iD} = u_i \qquad \forall i\in\mathcal{C} \tag{31}$$

$$\sum_{j\in\mathcal{C},j\neq i} y_{ji} + 1 = u_i \qquad \forall i\in\mathcal{C} \tag{32}$$

$$y_{ij} \geqslant x_{ij} \qquad \forall i,j\in\mathcal{C} \tag{33}$$

$$y_{ij} \leqslant (n-2)\cdot x_{ij} \qquad \forall i,j\in\mathcal{C} \tag{34}$$

$$y_{ij} + y_{ji} \geqslant u_j + (n-2)\cdot x_{ij} - (n-1)\cdot(1-x_{ji}) \qquad \forall i,j\in\mathcal{C} \tag{35}$$

$$y_{ij} + y_{ji} \leqslant u_j + x_{ji} - 1 \qquad \forall i,j\in\mathcal{C} \tag{36}$$

$$u_j \geqslant 2 - x_{Dj} + (n-3)\cdot x_{jD} \qquad \forall j\in\mathcal{C} \tag{37}$$

$$u_j \leqslant n-1-(n-3)\cdot x_{Dj} - 1 + x_{jD} \qquad \forall j\in\mathcal{C} \tag{38}$$

$$x_{ij}\in\{0,1\} \qquad \forall (i,j)\in\mathcal{E} \tag{39}$$

$$y_{ij}, u_i, l_{ij}\in\Re^{+} \qquad \forall i\in\mathcal{C},\quad (i,j)\in\mathcal{E} \tag{40}$$

The objective (28) is to minimize the total traveled distance. Constraints (29) and (30) assure that all nodes are visited exactly once. Subtours are avoided by (31)–(38).

Table 11
Notation used for the TSP formulation.

Parameters		Decision variables	
D	Central depot	$x_{ij} \in \{0,1\}$	Binary, 1 if vehicle traverses arc (i,j)
$\mathcal{C}$	Set of customers	$l_{ij} \in \Re^+$	Vehicle load on arc (i,j)
$\mathcal{V} = D \cup \mathcal{C}$	Set of vertices (including depot)	$u_i \in \Re^+$	Rank of node i (auxiliary routing variables)
$\mathcal{E} = \mathcal{V} \times \mathcal{V}$	Set of arcs	$y_{ij} \in \Re^+$	Rank of arc (i,j) in the tour
d_{ij}	Distance between $i \in \mathcal{V}$ and $j \in \mathcal{V}$		
q_i	Demand of customer $i \in \mathcal{C}$		
q^{total}	Total demand, $q^{total} = \sum_{i \in \mathcal{C}} q_i$		

$$[\text{TSP}^{\text{emis}}] \qquad \min \rightarrow \sum_{(i,j) \in \mathcal{E}} e(d_{ij}, m_{ij}, \bar{v}) \cdot x_{ij} \tag{41}$$

$$\sum_{j \in \mathcal{C}} l_{Dj} = q^{\text{total}} \tag{42}$$

$$l_{ij} \geqslant \sum_{k \in \mathcal{V}/\{i\}} l_{ki} - q_i - q^{\text{total}} \cdot (1 - x_{ij}) \qquad \forall (i,j) \in \mathcal{E} : i \neq D \tag{43}$$

$$l_{ij} \leqslant q^{\text{total}} \cdot x_{ij} \qquad \forall (i,j) \in \mathcal{E} \tag{44}$$

and (29)–(40).

The objective (41) of TSP^{emis} is to minimize the total emissions of the route, where function $e(d_{ij}, m_{ij}, \bar{v})$ yields the emissions for traveling along arc (i,j) as determined by (21). The emissions depend on the given speed $\bar{v}$ and the total vehicle weight $m_{ij} = m^{\text{tare}} + l_{ij}$ which is composed of the vehicle's empty weight m^{tare} and the load l_{ij} carried on arc (i,j). The load l_{ij} is initially set to the total customer demand $q^{\text{total}} = \sum_{i \in \mathcal{C}} q_i$, see (42). Constraint (43) then computes the load carried on each arc where (44) ensures that $l_{ij} = 0$ if $x_{ij} = 0$.

Note that the emissions in (41) depend on the chosen arcs (x_{ij}) and the moved loads (l_{ij}) which effects a non-linear objective function. We linearize (41) by inserting the energy definitions (7)–(10) into (21) and by exploiting that $x_{ij} = 0 \Rightarrow l_{ij} = 0$ due to Constraint (44), which finally yields the linear TSP^{emis} objective function

$$\begin{aligned} \min \rightarrow \sum_{(i,j) \in \mathcal{E}} & k \cdot \frac{d_{ij}}{v} \cdot r^{\text{idle}} \cdot x_{ij} + k \cdot \alpha \cdot d_{ij} \cdot c^{\text{roll}} \cdot g \cdot l_{ij} + k \cdot \alpha \cdot d_{ij} \cdot c^{\text{roll}} \cdot g \cdot m^{\text{tare}} \cdot x_{ij} \\ & + k \cdot \alpha \cdot \frac{1}{2000} \cdot c^{\text{air}} \cdot \rho \cdot A \cdot v^2 \cdot d_{ij} \cdot x_{ij} + k \cdot \alpha \cdot n^{\text{acc}} \cdot d_{ij} \cdot \left(\frac{0.504}{2 \cdot 3600} \cdot \left(m^{\text{tare}} \cdot x_{ij} + l_{ij} \right) \cdot v^2 \right) \end{aligned} \tag{45}$$

where $\alpha = \frac{r^{\text{full}} - r^{\text{idle}}}{P^{\text{vehicle}} \cdot \left(0.88 - 0.72 \cdot e^{-0.077 \cdot v^{1.41}}\right)}$.

References

André, M., 2004. Real-world driving cycles for measuring cars pollutant emissions – part a: the artemis european driving cycles.

Bektaş, T., Laporte, G., 2011. The pollution-routing problem. Transportation Research Part B: Methodological 45 (8), 1232–1250.

Black, I., Seaton, R., Ricci, A., Enei, R., 2003. Final Report: Actions to Promote Intermodal transport <http://www.transport-research.info/Upload/Documents/200607/20060727_155159_96220_RECORDIT_Final_Report.pdf> (accessed 02.06.04).

Boulter, P., McCrae, I., 2007. Assessment and Reliability of Transport Emission Models and Inventory Systems – Final Report <http://www.inrets.fr/ur/lte/publi-autresactions/fichesresultats/ficheartemis/report2/ARTEMIS_FINAL_REPORT.zip> (accessed 02.06.14).

De Haan, P., Keller, M., 2004. Modelling fuel consumption and pollutant emissions based on real-world driving patterns: the HBEFA approach. International Journal of Environment and Pollution 22 (3), 240–258.

Demir, E., Bektaş, T., Laporte, G., 2011. A comparative analysis of several vehicle emission models for road freight transportation. Transportation Research Part D: Transport and Environment 16 (5), 347–357.

Demir, E., Bektaş, T., Laporte, G., 2014. A review of recent research on green road freight transportation. European Journal of Operational Research 237 (3), 775–793.

EcoTransIT, 2014. Ecological Transport Information Tool for Worldwide Transports <http://www.ecotransit.org/> (accessed 02.06.14).

Edwards, R., Larivé, J.-F., Rickeard, D., Weindorf, W., 2014. Well-to-Wheels Analysis of Future Automotive Fuels and Powertrains in the European Context <http://iet.jrc.ec.europa.eu/about-jec/sites/iet.jrc.ec.europa.eu.about-jec/files/documents/report_2014/wtt_report_v4a.pdf> (accessed 02.06.14).

Franceschetti, A., Honhon, D., Woensel, T.V., Bektaş, T., Laporte, G., 2013. The time-dependent pollution-routing problem. Transportation Research Part B: Methodological 56 (0), 265–293.

Hausberger, S., Rexeis, M., Zallinger, M., Luz, R., 2009. Emission Factors from the Model PHEM for the HBEFA Version 3 <http://www.hbefa.net/d/documents/HBEFA_31_Docu_hot_emissionfactors_PC_LCV_HDV.pdf> (accessed 02.06.14), Techn. report, Technical University of Graz.

Hickman, J., Hassel, D., Joumard, R., Samaras., Z., Sorenson, S., 1999. Methodology for Calculating Transport Emissions and Energy Consumption <http://www.inrets.fr/ur/lte/cost319/M22.pdf> (accessed 02.06.14).

IBM, 2014. IBM ILOG CPLEX Optimizer <www.ilog.com/products/cplex> (accessed 02.06.14).

IPCC, 2006. 2006 IPCC Guidelines for National Greenhouse Gas Inventories <http://www.ipcc-nggip.iges.or.jp/public/2006gl/index.html> (accessed 02.06.14).

IPCC, 2007. Climate Change 2007 – The Physical Science Basis <https://www.ipcc-wg1.unibe.ch/publications/wg1-ar4/> (accessed 02.06.14).

IPCC, 2014. Climate Change 2014: Mitigation of Climate Change <http://mitigation2014.org/report/final-draft/> (accessed 02.06.14).

Jørgensen, M.W., Sorenson, S.C., 1997. Estimating Emissions From Railway Traffic. Report for the Project MEET: Methodologies for Estimating Air Pollutant Emissions From Transport.

Knörr, W., Seum, S., Schmied, M., Kutzner, F., Antes, R., 2010. Ecological Transport Information Tool for Worldwide Transports – Methodology and Data, 2nd Draft Report <http://www.ecotransit.org/download/EcoTransIT_World_Methodology_Data_100521.pdf> (accessed 02.06.14).
Kopfer, H.W., Schönberger, J., Kopfer, H., 2014. Reducing greenhouse gas emissions of a heterogeneous vehicle fleet. Flexible Services and Manufacturing Journal 26 (1-2), 221–248.
Kouridis, C., Gkatzoflias, D., Kioutsioukis, I., Ntziachristos, L., Pastorello, C., Dilara, P., 2011. Uncertainty Estimates and Guidance for Road Transport Emission Calculations <http://publications.jrc.ec.europa.eu/repository/bitstream/111111111/14202/1/uncertainty> Emisia SA, Thessaloniki.
Lindgreen, E., Sorenson, S.C., 2005a. Driving Resistance from Railroad Trains <http://www.inrets.fr/ur/lte/publi-autresactions/fichesresultats/ficheartemis/non_road4/Artemis_del7b_rail.pdf> (accessed 02.06.14), Techn. report, Technical University of Denmark, Lyngby.
Lindgreen, E., Sorenson, S.C., 2005b. Simulation of Energy Consumption and Emissions From Rail Traffic <http://www.inrets.fr/ur/lte/publi-autresactions/fichesresultats/ficheartemis/non_road4/Artemis_del7a_rail.pdf> (accessed 02.06.14), Techn. report, Technical University of Denmark, Lyngby.
McKinnon, A., Piecyk, M., 2010. Measuring and Managing CO_2 Emissions of European Chemical Transport <http://cefic-staging.amaze.com/Documents/IndustrySupport/Transport-and-Logistics/Sustainable> (accessed 02.06.14).
Nie, Y.M., Li, Q., 2013. An eco-routing model considering microscopic vehicle operating conditions. Transportation Research Part B: Methodological 55, 154–170.
Rakha, H., Lucic, I., 2002. Variable power vehicle dynamics model for estimating truck accelerations. Journal of Transportation Engineering 128 (5), 412–419.
Rakha, H.A., Ahn, K., Moran, K., Saerens, B., van den Bulck, E., 2011. Virginia Tech comprehensive power-based fuel consumption model: model development and testing. Transportation Research Part D: Transport and Environment 16 (7), 492–503.
Ramos, T.R.P., Gomes, M.I., Barbosa-Póvoa, A.P., 2014. Economic and environmental concerns in planning recyclable waste collection systems. Transportation Research Part E: Logistics and Transportation Review 62 (0), 34–54.
Rexeis, M., Hausberger, S., Riemersma, I., Tartakovsky, L., Zvirin, Y., van Poppel, M., Cornelis, E., 2005. Heavy Duty Vehicle Emissions – Final Report. Tech. rep., Graz University of Technology.
Ross, M., 1997. Fuel efficiency and the physics of automobiles. Contemporary Physics 38 (6), 381–394.
Schmied, M., Knörr, W., 2013. Berechnung von Treibhausgasemissionen in Spedition und Logistik gemäß DIN EN 16258. Tech. rep., DSLV Deutscher Speditions- und Logistikverband e.V.
Scora, G., Barth, M., 2006. Comprehensive Modal Emissions Model (CMEM), Version 3.01: User's Guide <http://cmscert.engr.ucr.edu/cmem/docs/CMEM_User_Guide_v3.01d.pdf> (accessed 02.06.14).
Sherali, H.D., Driscoll, P.J., 2002. On tightening the relaxations of Miller–Tucker–Zemlin formulations for asymmetric traveling salesman problems. Operations Research 50 (4), 656–669.
Solomon, M.M., 1987. Algorithms for the vehicle routing and scheduling problems with time window constraints. Operations Research 35 (2), 254–265.
Suzuki, Y., 2011. A new truck-routing approach for reducing fuel consumption and pollutants emission. Transportation Research Part D: Transport and Environment 16 (1), 73–77.